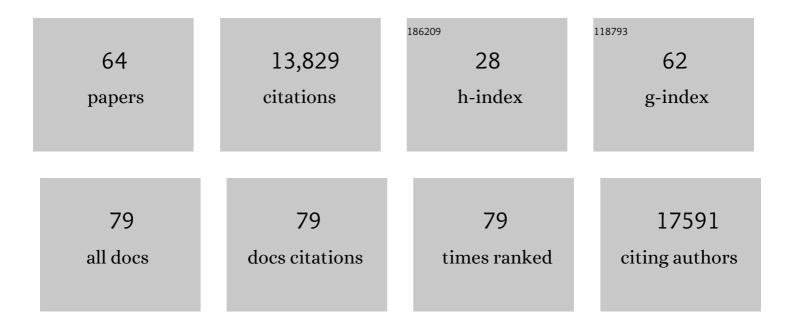
Tristan I Croll

List of Publications by Year in descending order

Source: https://exaly.com/author-pdf/4078419/publications.pdf Version: 2024-02-01



TDISTANLODOLL

#	Article	IF	CITATIONS
1	Catalytic trajectory of a dimeric nonribosomal peptide synthetase subunit with an inserted epimerase domain. Nature Communications, 2022, 13, 592.	5.8	16
2	Structural basis of SARS-CoV-2 Omicron immune evasion and receptor engagement. Science, 2022, 375, 864-868.	6.0	394
3	2.4-Ã structure of the double-ring <i>Gemmatimonas phototrophica</i> photosystem. Science Advances, 2022, 8, eabk3139.	4.7	16
4	How insulin-like growth factor I binds to a hybrid insulin receptor type 1 insulin-like growth factor receptor. Structure, 2022, 30, 1098-1108.e6.	1.6	16
5	The two-domain elevator-type mechanism of zinc-transporting ZIP proteins. Science Advances, 2022, 8, .	4.7	19
6	<scp>UCSF ChimeraX</scp> : Structure visualization for researchers, educators, and developers. Protein Science, 2021, 30, 70-82.	3.1	4,478
7	Phasertng: directed acyclic graphs for crystallographic phasing. Acta Crystallographica Section D: Structural Biology, 2021, 77, 1-10.	1.1	10
8	Adaptive Cartesian and torsional restraints for interactive model rebuilding. Acta Crystallographica Section D: Structural Biology, 2021, 77, 438-446.	1.1	16
9	Circulating SARS-CoV-2 spike N439K variants maintain fitness while evading antibody-mediated immunity. Cell, 2021, 184, 1171-1187.e20.	13.5	541
10	Molecular basis of ligand recognition and activation of human V2 vasopressin receptor. Cell Research, 2021, 31, 929-931.	5.7	38
11	Improving SARS-CoV-2 structures: Peer review by early coordinate release. Biophysical Journal, 2021, 120, 1085-1096.	0.2	21
12	Structure, Dynamics, Receptor Binding, and Antibody Binding of the Fully Glycosylated Full-Length SARS-CoV-2 Spike Protein in a Viral Membrane. Journal of Chemical Theory and Computation, 2021, 17, 2479-2487.	2.3	62
13	MyD88 TIR domain higher-order assembly interactions revealed by microcrystal electron diffraction and serial femtosecond crystallography. Nature Communications, 2021, 12, 2578.	5.8	55
14	Making the invisible enemy visible. Nature Structural and Molecular Biology, 2021, 28, 404-408.	3.6	18
15	SARS-CoV-2 RBD antibodies that maximize breadth and resistance to escape. Nature, 2021, 597, 97-102.	13.7	385
16	Cryo-EM structure of the monomeric <i>Rhodobacter sphaeroides</i> RC–LH1 core complex at 2.5â€Ã Biochemical Journal, 2021, 478, 3775-3790.	1.7	33
17	Structures of full-length glycoprotein hormone receptor signalling complexes. Nature, 2021, 598, 688-692.	13.7	52
18	Cryo-EM structure of the <i>Rhodospirillum rubrum</i> RC–LH1 complex at 2.5â€Ã Biochemical Journal, 2021, 478, 3253-3263.	1.7	23

TRISTAN I CROLL

#	Article	IF	CITATIONS
19	Ligand recognition and G-protein coupling selectivity of cholecystokinin A receptor. Nature Chemical Biology, 2021, 17, 1238-1244.	3.9	54
20	Cryo-EM Structure of the <i>Rhodobacter sphaeroides</i> Light-HarvestingÂ2 Complex at 2.1 Ã Biochemistry, 2021, 60, 3302-3314.	1.2	38
21	Cryo-EM structure of the dimeric <i>Rhodobacter sphaeroides</i> RC-LH1 core complex at 2.9â€Ã: the structural basis for dimerisation. Biochemical Journal, 2021, 478, 3923-3937.	1.7	26
22	Structure and ion-release mechanism of PIB-4-type ATPases. ELife, 2021, 10, .	2.8	8
23	Structures of fungal and plant acetohydroxyacid synthases. Nature, 2020, 586, 317-321.	13.7	37
24	Lig v 1 structure and the inflammatory response to the Ole e 1 protein family. Allergy: European Journal of Allergy and Clinical Immunology, 2020, 75, 2395-2398.	2.7	5
25	Developing a Fully Glycosylated Full-Length SARS-CoV-2 Spike Protein Model in a Viral Membrane. Journal of Physical Chemistry B, 2020, 124, 7128-7137.	1.2	240
26	How IGF-II Binds to the Human Type 1 Insulin-like Growth Factor Receptor. Structure, 2020, 28, 786-798.e6.	1.6	36
27	Structure of CD20 in complex with the therapeutic monoclonal antibody rituximab. Science, 2020, 367, 1224-1230.	6.0	113
28	Evaluation of templateâ€based modeling in CASP13. Proteins: Structure, Function and Bioinformatics, 2019, 87, 1113-1127.	1.5	56
29	Evaluation of model refinement in CASP13. Proteins: Structure, Function and Bioinformatics, 2019, 87, 1249-1262.	1.5	28
30	Cryo-EM structures of the pore-forming A subunit from the Yersinia entomophaga ABC toxin. Nature Communications, 2019, 10, 1952.	5.8	40
31	Molecular basis of cullin-3 (Cul3) ubiquitin ligase subversion by vaccinia virus protein A55. Journal of Biological Chemistry, 2019, 294, 6416-6429.	1.6	14
32	Macromolecular structure determination using X-rays, neutrons and electrons: recent developments in <i>Phenix</i> . Acta Crystallographica Section D: Structural Biology, 2019, 75, 861-877.	1.1	4,060
33	Xanthine Oxidoreductase: A Novel Therapeutic Target for the Treatment of Chronic Wounds?. Advances in Wound Care, 2018, 7, 95-104.	2.6	19
34	Automating tasks in protein structure determination with the clipper python module. Protein Science, 2018, 27, 207-216.	3.1	6
35	Design of <i>Plasmodium vivax</i> Hypoxanthine-Guanine Phosphoribosyltransferase Inhibitors as Potential Antimalarial Therapeutics. ACS Chemical Biology, 2018, 13, 82-90.	1.6	22
36	<i>ISOLDE</i> : a physically realistic environment for model building into low-resolution electron-density maps. Acta Crystallographica Section D: Structural Biology, 2018, 74, 519-530.	1.1	1,115

TRISTAN I CROLL

#	Article	IF	CITATIONS
37	Prediction of a novel internal rearrangement of the insulin receptor. Journal of Biomolecular Structure and Dynamics, 2017, 35, 857-867.	2.0	Ο
38	Multiple functional self-association interfaces in plant TIR domains. Proceedings of the National Academy of Sciences of the United States of America, 2017, 114, E2046-E2052.	3.3	103
39	Structural basis of TIR-domain-assembly formation in MAL- and MyD88-dependent TLR4 signaling. Nature Structural and Molecular Biology, 2017, 24, 743-751.	3.6	140
40	Improved Model of Proton Pump Crystal Structure Obtained by Interactive Molecular Dynamics Flexible Fitting Expands the Mechanistic Model for Proton Translocation in P-Type ATPases. Frontiers in Physiology, 2017, 8, 202.	1.3	29
41	A structural analysis of DNA binding by hSSB1 (NABP2/OBFC2B) in solution. Nucleic Acids Research, 2016, 44, 7963-7973.	6.5	26
42	Re-evaluation of low-resolution crystal structures <i>via</i> interactive molecular-dynamics flexible fitting (iMDFF): a case study in complement C4. Acta Crystallographica Section D: Structural Biology, 2016, 72, 1006-1016.	1.1	43
43	The CC domain structure from the wheat stem rust resistance protein Sr33 challenges paradigms for dimerization in plant NLR proteins. Proceedings of the National Academy of Sciences of the United States of America, 2016, 113, 12856-12861.	3.3	105
44	Antagonists of IGF:Vitronectin Interactions Inhibit IGF-l–Induced Breast Cancer Cell Functions. Molecular Cancer Therapeutics, 2016, 15, 1602-1613.	1.9	5
45	Higher-Resolution Structure of the Human Insulin Receptor Ectodomain: Multi-Modal Inclusion of the Insert Domain. Structure, 2016, 24, 469-476.	1.6	129
46	A preâ€clinical functional assessment of an acellular scaffold intended for the treatment of hardâ€ŧoâ€heal wounds. International Wound Journal, 2015, 12, 160-168.	1.3	7
47	The rate of <i>cis</i> – <i>trans</i> conformation errors is increasing in low-resolution crystal structures. Acta Crystallographica Section D: Biological Crystallography, 2015, 71, 706-709.	2.5	17
48	Transglutaminases and receptor tyrosine kinases. Amino Acids, 2013, 44, 19-24.	1.2	7
49	Vitronectin—Master controller or micromanager?. IUBMB Life, 2013, 65, 807-818.	1.5	76
50	Lysine residues of IGF-I are substrates for transglutaminases and modulate downstream IGF-I signalling. Biochimica Et Biophysica Acta - Molecular Cell Research, 2013, 1833, 3176-3185.	1.9	3
51	A peptidomimetic inhibitor of matrix metalloproteinases containing a tetherable linker group. Journal of Biomedical Materials Research - Part A, 2011, 96A, 663-672.	2.1	13
52	Modeling the adhesion of human embryonic stem cells to poly(lacticâ€≺i>coâ€glycolic acid) surfaces in a 3D environment. Journal of Biomedical Materials Research - Part A, 2010, 92A, 683-692.	2.1	13
53	Controlled presentation of recombinant proteins via a zinc-binding peptide-linker in two and three dimensional formats. Biomaterials, 2009, 30, 6614-6620.	5.7	11
54	Nanoscale presentation of cell adhesive molecules via block copolymer self-assembly. Biomaterials, 2009, 30, 4732-4737.	5.7	56

TRISTAN I CROLL

#	Article	IF	CITATIONS
55	Engineering tissue tubes using novel multilayered scaffolds in the rat peritoneal cavity. Journal of Biomedical Materials Research - Part A, 2008, 87A, 719-727.	2.1	15
56	Analysis of the Phase Behavior of the Aqueous Poly(ethylene glycol)-Ficoll System. Biotechnology Progress, 2008, 19, 1269-1273.	1.3	7
57	Transplantation of 3D scaffolds seeded with human embryonic stem cells: biological features of surrogate tissue and teratoma-forming potential. Regenerative Medicine, 2007, 2, 289-300.	0.8	68
58	Systematic selection of solvents for the fabrication of 3D combined macro- and microporous polymeric scaffolds for soft tissue engineering. Journal of Biomaterials Science, Polymer Edition, 2006, 17, 369-402.	1.9	41
59	A Blank Slate? Layer-by-Layer Deposition of Hyaluronic Acid and Chitosan onto Various Surfaces. Biomacromolecules, 2006, 7, 1610-1622.	2.6	137
60	Modelling oxygen diffusion and cell growth in a porous, vascularising scaffold for soft tissue engineering applications. Chemical Engineering Science, 2005, 60, 4924-4934.	1.9	74
61	Scaffolds, Stem Cells, and Tissue Engineering: A Potent Combination!. Australian Journal of Chemistry, 2005, 58, 691.	0.5	23
62	Production and Surface Modification of Polylactide-Based Polymeric Scaffolds for Soft-Tissue Engineering. , 2004, 238, 87-112.		28
63	Controllable Surface Modification of Poly(lactic-co-glycolic acid) (PLGA) by Hydrolysis or Aminolysis I:Â Physical, Chemical, and Theoretical Aspects. Biomacromolecules, 2004, 5, 463-473.	2.6	373
64	Quantitative prediction of phase diagrams for polymer partitioning in aqueous two-phase systems. Journal of Polymer Science, Part B: Polymer Physics, 2003, 41, 437-443.	2.4	3